Modeling the effect of 1 MeV electron irradiation on the performance of n^+p-p^+ Silicon space solar cells

Abdelghani Hammache[a], Nouredine Sengouga[a,*], Afak Meftah[a], Mohamed Henini[b]

[a] *Laboratory of Metallic and Semiconducting Materials (LMSM), Université de Biskra, BP 455 RP, 07000 Biskra, Algeria.*

[b] *School of Physics and Astronomy, Nottingham Nanotechnology and Nanoscience Center, University of Nottingham, Nottingham, NG7 2RD, UK*

[*] Corresponding author n.sengouga@univ-biskra.dz (N. Sengouga)

ABSTRACT

Energetic particles such as electrons and protons induce severe degradation on the performance of solar cells used to power satellites and space vehicles. This degradation is usually attributed to lattice damage in the active region of the solar cell. One of the phenomena observed in silicon solar cells exposed to 1 MeV electron irradiation is the anomalous degradation of the short circuit current (J_{SC}). It initially decreases followed by a recovery before falling again with increasing electron fluence. This behavior is usually attributed to type conversion of the solar cell active region. The other figures of merit, on the other hand, decrease monolithically. In this work numerical simulator SCAPS (Solar Cell Capacitance Simulator) is used to elucidate this phenomenon. The current-voltage (J-V) characteristics of a Si n^+-p-p^+ structure are calculated under AM0 with the fluence of 1MeV electrons as a variable parameter. The effect of irradiation on the solar cell is simulated by a set of defects of which the energy levels lie deep in energy gap of silicon. Although several types of deep levels are induced by irradiation including deep donors (DD), deep acceptors (DA) and/or generation-recombination centers (GRC), it was found that, only one of them (the shallowest donor) is responsible for the anomalous degradation of J_{SC}. It will be also shown, by calculating the free charge carrier profile in the active region, that this behavior is not related to type conversion but to a widening of the space charge region.

Keywords: Si solar cells; 1 MeV electron irradiation; short circuit current; numerical simulation; SCAPS.

1. Introduction

For satellites and space vehicles, the only source of energy is photovoltaic solar cells. Materials that can be used to make solar cells for this purpose have to withstand harsh conditions that include high temperatures and energetic particles. Only a few materials such as Si and some III-V semiconductors and their alloys (GaAs, InP and GaInP) can meet these conditions [1, 2]. Good quality crystals with well controlled doping can be easily achieved due to the mature technology of these semiconductors. Compound semiconductors are preferred because of their higher conversion efficiencies and radiation-resistance, but silicon still has a better cost effectiveness and reliability. The solar cells used in space are subjected to charged particles such as protons and electrons of a wide energy range. The highly energetic particles interacting with solar cells induce defects in the semiconductor lattice and, consequently, deteriorate the solar cell performance [3]. The performance degradation of solar cells subjected to energetic electrons and protons in laboratories is well characterized [4-9]. It was observed that the space solar figures of merit (the short circuit current I_{SC}, the open circuit voltage V_{OC}, the maximum output power P_{MAX} , the fill factor FF and the conversion efficiency η) decrease linearly with the logarithm of the fluence. The degradation was analytically modeled [10-14] in order to predict the effect of the long term exposure of the solar cells [15, 16]. For example, P_{MAX} is related to the irradiation fluence by a simple formula of the form [17]:

$$P_{MAX}(\varphi) = P_0\left(1 - C\ln\frac{\varphi}{\varphi_0}\right) \qquad (1)$$

where φ is the irradiation fluence, φ_0 is the fluence threshold for the power reduction, P_0 is the pre-irradiated maximum output power and C is a fitting constant. The other figures of merit follow a similar pattern, in most cases, which means that they decrease monolithically with increasing fluence. However, in some silicon solar cells, the short circuit current does not strictly follow this behavior. Instead, it initially decreases, then at a certain fluence it slightly increases before decreasing again sharply [2, 5, 7, 9, 13-14, 18-19]. This slight recovery of the short circuit current is usually attributed to a type conversion of the base (from n to p-type for example) [20]. Among the defects created by irradiation are compensating centers which

reduce the initial doping density. They are responsible of a phenomenon known as carrier removal, which is modeled by an analytical expression [14] expressed by:

$$p_\varphi = p_0 exp\left(-\frac{R_C \varphi}{p_0}\right) \qquad (2)$$

p_0 is the initial hole density (post-irradiated p-type Si) and R_C is the removal rate.

The analytical modeling of the anomalous degradation of the short circuit current divides the $I_{SC}(\varphi)$ curve into four regions [2, 5, 7, 14, 18]. The first region is just for $\varphi < \varphi_0$, i.e. when I_{SC} is still not affected by φ. In this region the created defects have negligible densities compared to shallow doping. The second region is when the short circuit decreases with increasing fluence. This is explained by a decrease in the minority carrier lifetime and hence in their diffusion length. The dependence of I_{SC} on the diffusion length L and the space charge region width W is roughly given by:

$$I_{SC} = qF\{1 - \exp(-\alpha W)/(1 + \alpha L)\} \qquad (3)$$

α is the absorption coefficient and F is the photon flux.

The third region is when the short circuit increases with increasing fluence. This is related to the onset of the type conversion where the space charge width increases instead of decreasing. Therefore the short circuit current increases according to equation (3). The fourth region is when the short circuit falls sharply with increasing fluence. This is explained by the increase in the base resistivity associated with the decrease in carrier concentration due to compensation by deep defects. Another work by Karazhanov [13] assumed a simplified model in which the free carriers (holes) are compensated by a single donor deep level. The conversion of the p-type semiconductor to n-type is reached when the deep level concentration surpasses that of holes. This leads to an increase in the short circuit current, also according to equation (3).

In the above analysis several simplifications were made. In particular, the defects created by irradiation are assumed to act as one effective deep level. In reality and as it is well known, irradiation creates several defects of different types: GRCs, DDs and DAs [21-26]. Experimentally it is not always easy to distinguish GRs from DDs and DAs. This means that analytical modeling cannot clearly link the observed degradation of the solar cell figures of merit to a particular defect. On the other hand numerical simulation has the ability of unequivocally relating the degradation of each figure of merit to a particular defect [27-33]. In the present work, it can reveal which defect is responsible for the observed phenomenon (the

anomalous behavior of the short circuit current) in Si solar cells. It can also evaluate the behavior of internal parameters such as the free carrier concentration so that they can be used to explain the observed effect. Numerical simulation is carried out using the software SCAPS (Solar Cell Capacitance Simulator) developed by M. Burgelman and co-workers at the Department of Electronics and Information Systems (ELIS) of the University of Gent, Belgium [34].

2. Simulation

The current-voltage characteristics of the solar cell are calculated using the software SCAPS. SCAPS is a Windows application program, organized in a number of panels, in which the user can set the parameters. The program opens with an `action panel', where the user can set an operating point (temperature, voltage, frequency, illumination), and an action list of calculations to carry out (J-V, C-V, C-f, Q(λ)). In each calculation, the running parameter (V, f or λ) is varied in the specified range, whilst all other parameters have the values specified in the operation point. Also, the user can directly view previously calculated results, namely J-V, C-V, C-f, Q(λ), and also band diagrams, electric field, carrier densities, partial recombination currents.

Like any numerical simulation, SCAPS solves the basic semiconductor equations which are: the Poisson equation, relating the charge to the electrostatic potential ψ, and the continuity equations for electrons and holes. In one dimension, the total cell length L is divided into N intervals, and the value of ψ_i and the electron and hole concentrations n_i and p_i at each of the intervals constitute the unknowns of the problem. They can be found by numerically solving 3N non-linear equations, i.e. the basic equations at each of the intervals i. Alternatively, one can choose ψ_i, ϕ_n and ϕ_p as independent variables instead of (ψ_i, n_i, p_i). Here ϕ_n and ϕ_p are the quasi-fermi energy levels for electrons and holes respectively. The basic equations are non-linear because the continuity equations contain a recombination term, which is non-linear in n and p.

The simplest and useful model of charge transport is the Drift-Diffusion Model. This model, which is based on the two first equations cited above, is adequate for nearly all devices that were technologically feasible. The Poisson's equation which relates the electrostatic potential to the space charge density is given by:

$$\varepsilon \frac{d^2\psi}{dx^2} = -\rho(x) \tag{4}$$

where ψ is the electrostatic potential, ε is the local permittivity, and ρ is the local space charge density.

The continuity equations in steady state for electrons and holes are expressed, respectively by:

$$0 = \frac{1}{q}\frac{dJ_n}{dx} + G_n - R_n \tag{5.a}$$

$$0 = -\frac{1}{q}\frac{dJ_p}{dx} + G_p - R_p \tag{5.b}$$

where n and p are the electron and hole concentration, $\overrightarrow{J_n}$ and $\overrightarrow{J_p}$ are the electron and hole current densities, G_n and G_p are the generation rates for electrons and holes, R_n and R_p are the recombination rates for electrons and holes, and q is the electron charge.

In the drift-diffusion model, the current densities are expressed in terms of the quasi-Fermi levels ϕ_n and ϕ_p as:

$$\vec{J}_n = -q\mu_n n \frac{\mathrm{d}\phi_n}{\mathrm{dx}} \tag{6.a}$$

$$\vec{J}_p = -q\mu_p p \frac{\mathrm{d}\phi_p}{\mathrm{dx}} \tag{6.b}$$

where μ_n and μ_p are the electron and hole mobilities, respectively. The quasi-Fermi levels are linked to the carrier concentrations and the potential through the two Boltzmann approximations:

$$n = n_i exp\left(\frac{\psi - \phi_n}{k_B T}\right) \tag{7.a}$$

$$p = n_i exp\left(-\frac{\psi - \phi_p}{k_B T}\right) \tag{7.b}$$

where n_i is the effective intrinsic concentration and T is the lattice temperature.

The electrical characteristics are calculated following the specified physical structure and bias conditions. This is achieved by approximating the operation of the device into a one-dimensional grid, consisting of a number of grid points called nodes. By applying the set of differential equations (Poisson's and continuity equations) onto this grid (or equation's

discretization), the transport of carriers through the structure can be simulated. The finite element grid is used to represent the simulation domain.

The Si solar cell used in this work is similar to that of [35]. It is a typical 50 μm thick n^+-p-p^+ structure used for space applications. The different parameters of this solar cell are presented in Table 1. A two-dimensional schematic view of the solar cell is shown in Fig. 1.

Table 1. The parameters of the Si n+-p-p+ solar cell simulated in this work.

	Thickness (μm)	Doping density (cm^{-3})	Type
Emitter	0.15	1×10^{19}	n^+
Base	49.70	1×10^{15}	P
Back surface field region	0.15	5×10^{18}	p^+

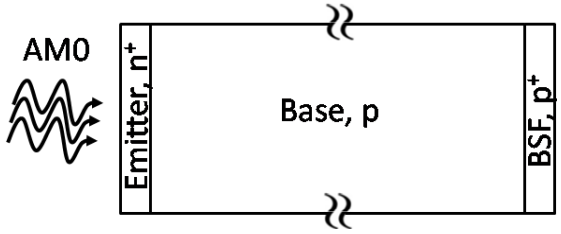

Fig. 1. A two-dimensional schematic view of the Si n^+-p-p^+ solar cell. BSF is the back surface field.

The emitter side of the solar cell (n^+) is illuminated by AM0 spectrum and the J-V characteristics are calculated for different fluences of 1MeV electrons. Irradiation by these energetic particles creates defects in the Si lattice, which manifest as recombination centers or traps for free carriers. A lot of work is carried out to characterize these defects so that a large number of defects are detected in Si. For simplicity we have used the most common observed defects [1, 18]. These are summarized in Table 2.

Table 2. The parameters of the commonly detected defects in Si solar cells irradiated by 1 MeV electrons [1, 18]. Introduction rate, k is the proportionality factor between the trap density and the fluence ($k = N_T/\varphi$).

Activation energy (eV)	Capture cross section, σ (cm^2)	Introduction rate, k (cm^{-1})	Trap type
$E_V + 0.18$	3.1×10^{-15}	0.002	Majority
$E_V + 0.36$	6.2×10^{-15}	0.016	Majority
$E_C - 0.20$	9.9×10^{-15}	0.002	Minority
$E_V + 0.56$	6.3×10^{-13}	0.004	Majority
$E_C - 0.71$	3.55×10^{-13}	0.004	Minority

3. Results and discussions

Since the solar cell used in this work has an n^+-p-p^+ structure, it is expected that the defects will be mainly created within the thickest region which is the p-type base where the majority traps are hole traps while electron traps are the minority traps. Hence the majority traps will only contribute to the reduction of the minority carrier lifetime but not to the shallow doping compensation. It is therefore the minority traps which will be responsible for this phenomenon. Referring to Table 2, there are only two minority traps: $E_C - 0.20$ and $E_C - 0.71\ eV$. The second, the deepest, is only observed when the electron irradiation fluence surpasses the critical value where the short circuit current shows the anomalous behavior. In order to establish which trap is responsible the J-V characteristics are calculated under the effect of each minority (donor-like) trap. Obviously, the majority traps are all taken into account in both cases. It has to be also mentioned that, in numerical simulation, several possibilities may be considered: the two minority traps are considered separately, then together and in each case the trap parameters are adjusted to reproduce the experimental behavior.

First when the two traps are taken individually with their parameters given in Table 2 and then together, the calculated J-V characteristics under different fluences are shown in Fig. 2 a, b and c for the shallower, $E_C - 0.20\ eV$, the deeper, $E_C - 0.71\ eV$, traps and together, respectively.

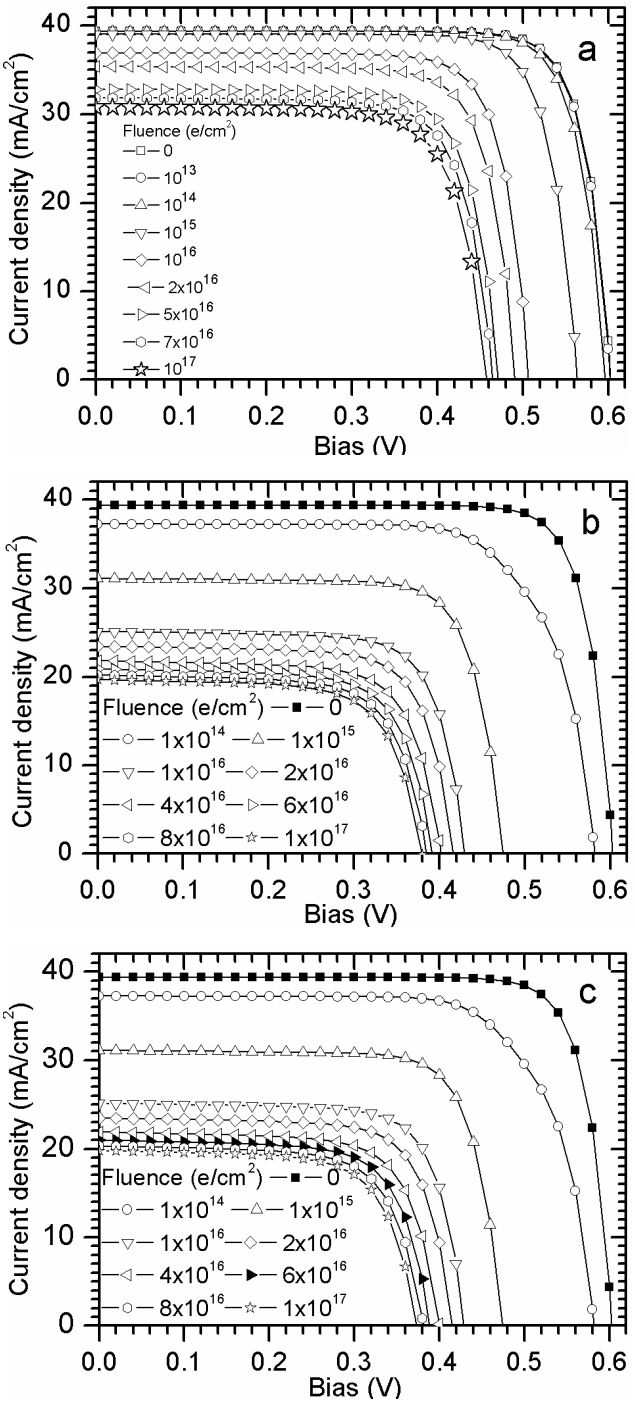

Fig. 2. The calculated J-V characteristics of the n^+-p-p^+ Si solar cell under AM0 for different fluences of 1 MeV electron irradiation taking into account the majority traps with the minority traps individually: (a) the shallower minority trap, $E_C - 0.20\ eV$; (b) the deeper minority trap, $E_C - 0.71\ eV$; and (c) the two minority traps together.

From these characteristics, the figures of merit of solar cell are extracted. The remaining parameters after irradiation (normalized to their initial pre-irradiated values) are shown in Fig.

3 for case (a). Cases (b) and (c) are similar in the behavior and differ only in the magnitude). Thus the experimentally observed behavior is not reproduced.

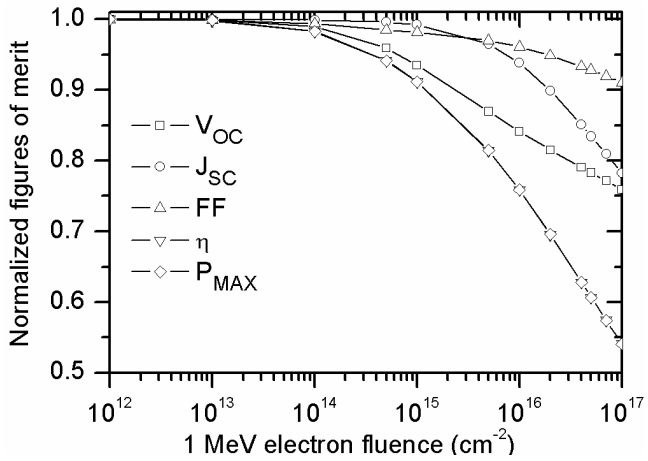

Fig. 3. The effect of 1 MeV electron irradiation on the figures of merit of the n^+-p-p^+ Si solar cell under AM0, extracted from the calculated J-V characteristics (Fig. 1-a-) and normalized to the pre-irradiated value, taking into account all acceptor traps and the shallower donor trap ($E_C - 0.20\ eV$).

It is clear that in all cases both the short circuit current and the open circuit voltage decrease with increasing fluence of electron irradiation. The maximum available power and the conversion efficiency follow the same pattern. However the fill factor (FF) does not change appreciably. Since the experimental observed behavior is not reproduced in the previous cases, we will have to change some of the parameters of the minority traps since they are responsible for the so-called type conversion. The suggested parameter changes may be justified by the fact that it is not easy to characterize precisely so many traps present in one sample even by the most powerful techniques as demonstrated in some of our previous work [27]. Amongst all the trap parameters, usually the introduction rate is the most difficult to evaluate precisely by DLTS (Deep Level Transient Spectroscopy), for example, which is the most commonly used technique in the characterization of traps. For this reason, we chose to use the introduction rate as a fitting parameter. It was found that only when changing the introduction rate of the shallower minority tarp ($E_C - 0.20\ eV$) from 0.002 to 0.04 that the phenomenon can be reproduced. The J-V characteristics in this case are presented in Fig. 4. It has to be mentioned here that changing the introduction rate of the deeper minority trap ($E_C - 0.71\ eV$) did not reproduce the desired phenomenon.

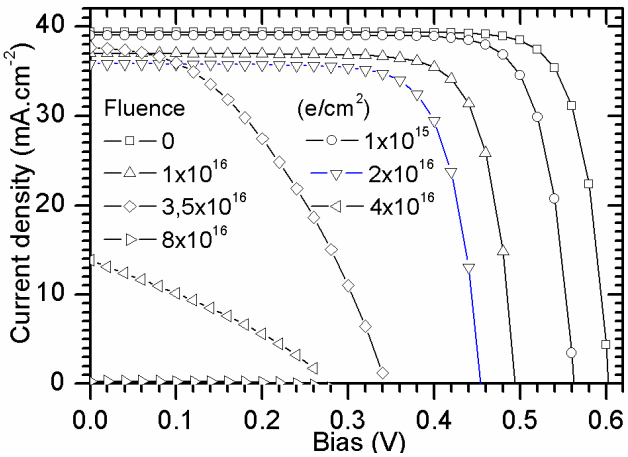

Fig. 4. The calculated J-V characteristics of the n^+-p-p^+ Si solar cell under AM0 for different fluences of 1 MeV electron irradiation by changing the introduction rate of the shallower minority tarp ($E_C - 0.20\ eV$) from 0.002 to 0.04 but excluding the deeper minority trap ($E_C - 0.71\ eV$).

It is very clear that there is a big difference as compared with the J-V characteristics shown in Fig. 2. There are two main differences. First the fill factor is hugely affected in contrast to the previous case. Second, the other figures of merit all decrease monolithically with increasing electron fluence except the short circuit current which decreases then increases at a certain fluence before it decreases abruptly again . To see this phenomenon even clearly, the short circuit current is extracted from the J-V characteristics. It is then normalized to the un-irradiated value and is presented in Fig. 5.

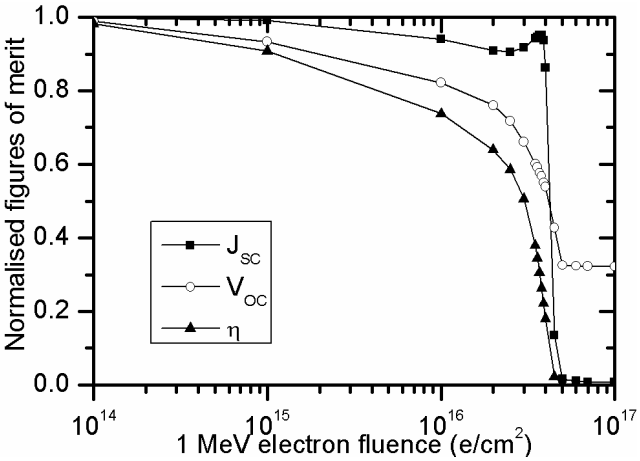

Fig.5 . The extracted short circuit current, normalized to the unirradiated value, from the calculated J-V characteristics (Fig. 4) of the n^+-p-p^+ Si solar cell under AM0 for different fluences of 1 MeV electron irradiation by changing the introduction rate of the shallower

minority tarp ($E_C - 0.20\ eV$) from 0.002 to 0.04 but excluding the deeper minority trap ($E_C - 0.71\ eV$).

Although the shape of the experimentally observed phenomenon is reproduced but the steepness of its degradation is not. In fact the short circuit degradation is less than 10 % before the appearance of the anomalous phenomenon. The measured degradation is ~20 %. In the following the deeper minority trap ($E_C - 0.71\ eV$) is taken into account and the calculated J-V characteristics in this case are shown in Fig. 6.

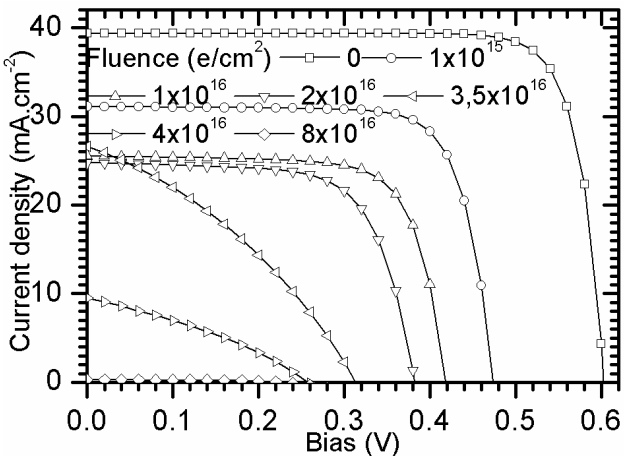

Fig. 6. The calculated J-V characteristics of the n^+-p-p^+ Si solar cell under AM0 for different fluences of 1 MeV electron irradiation by changing the introduction rate of the shallower minority tarp ($E_C - 0.20\ eV$) from 0.002 to 0.04 but including the deeper minority trap ($E_C - 0.71\ eV$).

It can be seen that the J-V characteristics are more affected. To visualize this larger impact the figures of merit are extracted from the J-V characteristics, normalized and shown in Fig.7.

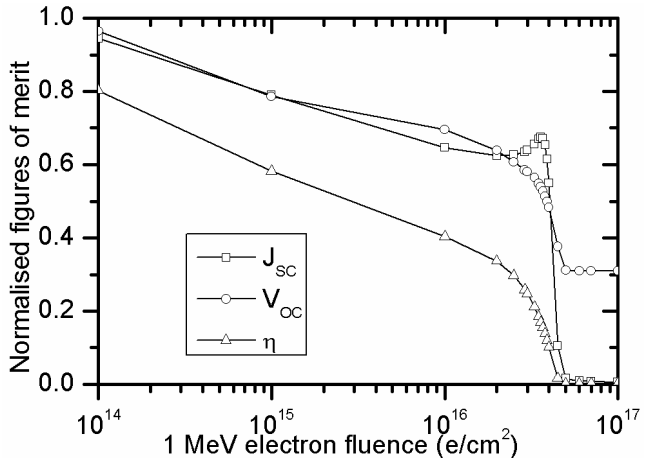

Fig.7 . The extracted short circuit current, normalized to the unirradiated value, from the calculated J-V characteristics (Fig. 6) of the n^+-p-p^+ Si solar cell under AM0 for different fluences of 1 MeV electron irradiation by changing the introduction rate of the shallower minority tarp ($E_C - 0.20\ eV$) from 0.002 to 0.04 but including the deeper minority trap ($E_C - 0.71\ eV$).

In this figure it can be clearly seen that the degradation rate increases and is comparable to values obtained experimentally [1, 17]. It is also worth mentioning that the fluence at which this phenomenon appears is very comparable to measurements.

As it was mentioned previously, the anomalous degradation of the short circuit current is usually related to type conversion of the active region of the solar cell (base) by several authors as detailed in section 1. The argument was mainly qualitative and no clear cut evidence was presented. In this work it will be shown that type conversion is not responsible for this phenomenon. For this purpose the electron and hole density distribution in the whole solar cell change with the 1 MeV electron fluence is evaluated corresponding to the region where the short circuit current shows the anomalous behavior.. This is shown in Fig. 8.

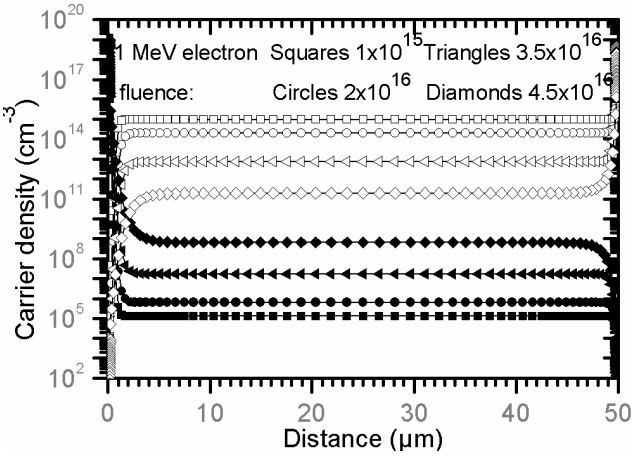

Fig. 8. The electron (solid symbols) and the hole densities distribution along the n^+-p-p^+ Si solar cell structure for different fluences of 1 MeV electron irradiation corresponding to the region where the short circuit current shows the anomalous behavior.

The hole density decreases and the electron density increases with increasing the fluence but the first never surpasses the second although the fluence is larger than the threshold for the

short circuit current increase, which is $\approx 2 \times 10^{16}\ e/cm^2$ (see Fig. 7). This means that the base is still p-type and hence the type conversion is not achieved. It is worth pointing out here that numerical simulation has an advantage over experimental characterization and analytical modeling since it can evaluate the internal parameters of the structure such as the electron and hole densities. Such evaluation cannot be realized by experimental characterization and analytical modeling. In order to explain the anomalous behavior of the short circuit current we will study the evolution of the depletion region (W). The first parameter can be roughly evaluated from Fig. 8. For this purpose the left side of Fig. 8 is magnified to show the depletion region of the p-n^+ junction and is shown in Fig. 9.

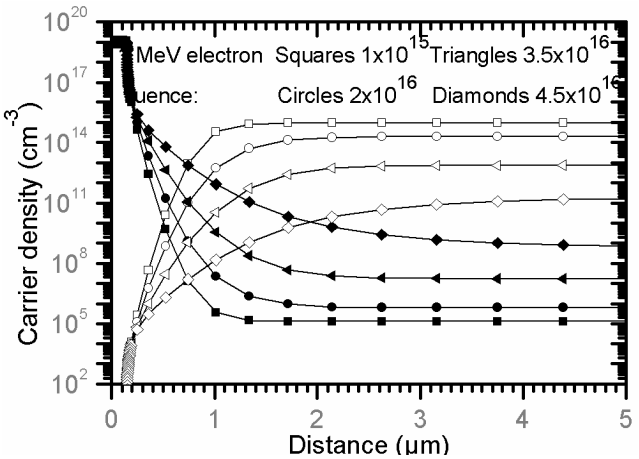

Fig. 9. Enlargement of the left side of Fig. 8 to show the depletion region at the n^+-p junction (right side) of the n^+-p-p^+ solar cell.

As the fluence, corresponding to the region where the short circuit current shows the anomalous behavior, increases the depletion region width increases since the hole density decreases. This will lead to an increase in the short circuit current according to equation (3).

4. Conclusion

Numerical simulation using the software SCAPS was carried out to study the effect of 1 MeV electron irradiation of an n^+-p-p^+ Si solar cell under AM0. Irradiation induces structural defects in the Si lattice. These defects introduce energy levels in the Si forbidden energy gap and which act as recombination centers and/or traps of free carriers. The solar cell performance suffers a severe deterioration as a result. We have concentrated on the

anomalous behavior of the short circuit current. To elucidate this effect, the J-V characteristics were calculated taking into consideration the minority traps separately, and together with all the majority carriers. It was concluded that a shallower minority trap is responsible for the phenomenon while the deeper minority trap enhances this phenomenon. It was found that this phenomenon is not related to the type conversion phenomenon.

References

[1] M. Yamaguchi, Radiation-resistant solar cells for space use, Solar Energy Materials & Solar Cells 68 (2001) 31-53.

[2] J.C. Bourgoin, N. de Angelis, Radiation-induced defects in solar cell materials, Solar Energy Materials & Solar Cells 66 (2001) 467-477.

[3] J.C. Bourgoin, R. Kiliulis, C. Gonzales, G. Strob, C. Flores, K. Bogus, C. Signorini, Deep space degradation of Si and GaAs solar cells, 25th PVSC; May 13-17, 1996; Washington, D.C.

[4] G.H. Shin, K.S. Ryu, H. M. Kim, K. W. Min, Radiation Effect Test for Single-Crystalline and Polycrystalline Silicon Solar Cells, J. Korean Physical Soc.52 (2008) 843-847.

[5] M. Imaizumi, S. J. Taylor, M. Yamaguchi, T. Ito, T. Hisamatsu, S. Matsuda, Analysis of structure change of Si solar cells irradiated with high fluence electrons, J. Appl. Phys. 85 (1999) 1916-1920..

[6] B. Danilchenko, A. Budnyk, L. Shpinar, D. Poplavskyy, S.E. Zelensky, K.W.J. Barnham, N.J. Ekins-Daukes, 1MeV electron irradiation influence on GaAs solar cell performance, Solar Energy Materials & Solar Cells 92 (2008) 1336–1340.

[7] M. Yamaguchi, S. J. Taylor, M. J. Yang, S. Matsuda, O. Kawasaki, T. Hisamatsu, High-energy and high-fluence proton irradiation effects in silicon solar cells, J. Appl. Phys. 80 (1996) 4916-4920.

[8] M. Hadrami , L. Roubi, M. Zazoui, J. C. Bourgoin, Relation between solar cell parameters and space degradation, Sol. Energy Mater. Sol. Cells, 90 (2006) 1486–1497.

[9] M. Yamaguchi, A. Khan, S. J. Taylor, M. Imaizumi, T. Hisamatsu, S. Matsuda, A Detailed Model to Improve the Radiation-Resistance of Si Space Solar Cells, IEEE Trans. Electron Dev. 46 (1999) 2133-2138..

[10] J. H. Warner, S. R. Messenger, R. J. Walters, G. P. Summers, J. R. Lorentzen, D. M. Wilt, M. A. Smith,Correlation of electron radiation induced-damage in GaAs solar cells, IEEE Trans. Nucl. Sci. 53 (2006) 1988–1994.

[11] M. Alurralde, M. J. L. Tamasi, C. J. Bruno, M. G. M. Bogado, J. Plá, J. F. Vázquez, J. Durán, J. Schuff, A. A. Burlon, P. Stoliar,, A. J. Kreiner, Experimental and theoretical radiation damage studies on crystalline silicon solar cells, Solar Energy Materials & Solar Cells 82 (2004) 531–542.

[12] S. Makham and G.C.Sun,J.C.Bourgoin, Modelling of solar cell degradation in space, Solar Energy Materials & Solar Cells 94 (2010) 971–978.

[13] S. Z. Karazhanov, Mechanism for the anomalous degradation of proton- or electron-irradiated silicon solar cells, Solar Energy Materials & Solar Cells 69 (2001) 53-60.

[14] M. Yamaguchi, S. J. Taylor, S. Matsu, O. Kawasaki, Mechanism for the anomalous degradation of Si solar cells induced, by high fluence 1 MeV electron irradiation, Appl. Phys. Lett. 68 (1996) 3141-3143.

[15] S. Makham, M. Zazoui, G.C. Sun, J.C. Bourgoin, Prediction of proton-induced degradation of GaAs space solar cells, Solar Energy Materials & Solar Cells 90 (2006) 1513–1518.

[16] M. Mbarki, G. C. Sun, J. C. Bourgoin, Prediction of solar cell degradation in space from the electron–proton equivalence, Semicond. Sci. Technol. 19 (2004) 1081–1085.

[17] R. J. Walters, M. A. Xapsos, G. P. Summers, Radiation response of single and dual junction p+-n InGaP/GaAs space solar cells, Proceedings of the 26th IEEE Photovoltaic Specialist Conference, 29 September–03 October 1997, Anaheim, CA,1997, pp.843–846.

[18] M. Yamaguchi A. Khan, S. J. Taylor, K. Ando, T. Yamaguchi, S. Matsuda,T, Aburaya, Deep level analysis of radiation-induced defects in Si crystals and solar cells, J. Appl. Phys. 86 (1999) 217-223.

[19] N. de Angelis, J.C. Bourgoin, T. Takamoto, A. Khan and M. Yamaguchi, Solar cell degradation by electron irradiation. Comparison between Si, GaAs and GaInP cells, Solar Energy Materials & Solar Cells 66 (2001) 495-500.

[20] S. J. Taylor, M. Yamaguchi, M. J. Yang, M. Imaizumi, S. Matsuda, O. Kawasaki, T. Hisamatsu, Type conversion in irradiated silicon diodes, Appl. Phys. Lett. 70 (1997) 2165-2167.

[21] X. Xiang, W. Du, X. Chang and X. Liao , Electron irradiation and thermal annealing effect on GaAs solar cells, Solar Energy Materials & Solar Cells 55 (1998) 313-322.

[22] A. Khan, M. Yamaguchi, T. Aburaya and S. Matsuda, Comparison of the effects of electron and proton irradiation on type-converted silicon space solar cells upon annealing, Semicond. Sci. Technol. 15 (2000) 403–407.

[23] C. A. Londos and P.C. Banbury, Defect studies in electron-irradiated boron-doped silicon, J. Phys. C: Solid State Phys. 20 (1987) 645-650.

[24] N. Chandrasekaran, T. Soga, Y. Inuzuka, M. Imaizumi, H. Taguchi and T. Jimbo, 1MeV electron irradiation effects of GaAs/Si solar cells, Mater. Res. Soc. Symp. Proc 836 (2005) L6.7.1-6.

[25] A. Khan, M. Yamaguchi, T. Takamoto, N. de Angelis and J.C. Bourgoin, Recombination centers in electron irradiated GaInP: application to the degradation of space solar cells, Journal of Crystal Growth 210 (2000) 264-267.

[26] T. Hisamatsu, T. Matsuda, T. Nakao, Y. Matsumoto, S. J. Taylor and M. Yamaguchi, Thermal recovery of degraded space silicon solar cells due to large fluence irradiation, 26th PVSC; Sept. 30-0ct. 3,1997; Anaheim, CA, 991-4.

[27] A. Ali, T. Gouveas, M. A. Hasan, S. H. Zaidi, M. Asghar, Influence of deep level defects on the performance of crystalline silicon solar cells: Experimental and simulation study, Solar Energy Materials & Solar Cells 95 (2011) 2805 –2810

[28] A F Meftah, N Sengouga, A Belghachi and A M Meftah, Numerical simulation of the effect of recombination centres and traps created by electron irradiation on the performance degradation of GaAs solar cells, J. Phys.: Condens. Matter 21 (2009) 215802-215809.

[29] A.F. Meftah, N. Sengouga, A.M. Meftah , S. Khelifi, Numerical simulation of the effect of the Al molar fraction and thickness of an $Al_xGa_{1-x}As$ window on the sensitivity of a p^+–n–n^+ GaAs solar cell to 1 MeV electron irradiation, Renewable Energy 34 (2009) 2426-2431.

[30] A.F. Meftah, N. Sengouga, A.M. Meftah, A. Belghachi, Detailed numerical simulation of the effect of defects created by electron irradiation on the performance degradation of a p^+–n–n^+ GaAs solar cell, Renewable Energy 34 (2009) 2422–2425.

[31] AF. Meftah, AM. Meftah, N. Sengouga, S. Khelifi, The $Al_xGa_{1-x}As$ window composition effect on the hardness improvement of a p^+–n–n^+ GaAs solar cell exposed to the electron irradiation, Energy Conversion and Management 51 (2010) 1676–1678.

[32] W. Laiadi, AF. Meftah, N. Sengouga and AM. Meftah, Irradiation effect on the electrical characteristics of an AlGaAs/GaAs based solar cell: Comparison between electron and proton irradiation by numerical simulation, Superlattices and Microstructures 58 (2013) 44–52.

[33] M A Cappelletti, G A Casas, A P Cédola and E L Peltzer y Blancá, Theoretical study of the maximum power point of n-type and p-type crystalline silicon space solar cells, Semicond. Sci. Technol. 28 (2013) 045010-045017.

[34] M. Burgelman, P. Nollet and S. Degrave, Modelling polycrystalline semiconductor solar cells, Thin Solid Films 361-362 (2000) 527-532.

[35] T. Hisamatsu, O. Kawasaki, S. Matsuda, T. Nakao and Y. Wakow, Radiation degradation of large fluence irradiated space silicon solar cells, Solar Energy Materials and Solar Cells 50 (1998) 331-338.